Performance of closely spaced point absorbers with constrained floater motion

G. De Backer[1], M. Vantorre[1], C. Beels[1], J. De Rouck[1] and P. Frigaard[2]

[1]Department of Civil Engineering,
Ghent University,
Technologiepark Zwijnaarde, 9052 Zwijnaarde, Belgium
E-mail: griet.debacker@ugent.be

[2]Department of Civil Engineering,
Aalborg University,
Sohngaardsholmsvej 57, 9000 Aalborg, Denmark
E-mail: i5pf@civil.aau.dk

Abstract

The performance of a wave energy converter array of twelve heaving point absorbers has been assessed numerically in a frequency domain model. Each point absorber is assumed to have its own linear power take-off. The impact of slamming, stroke and force restrictions on the power absorption is evaluated and optimal power take-off parameters are determined. For multiple bodies optimal control parameters are not only dependent on the incoming waves, but also on the position and behaviour of the other buoys. Applying the optimal control values for one buoy to multiple closely spaced buoys results in a suboptimal solution, as will be illustrated. Other ways to determine the power take-off parameters are diagonal optimization and individual optimization. The latter method is found to increase the power absorption with about 14% compared to diagonal optimization.

Keywords: array, constraints, multiple bodies, point absorber, wave energy

Nomenclature

b_{ext}	=	external damping coefficient [kg/s]
B_{ext}	=	external damping matrix (NxN) [kg/s]
B_{hyd}	=	hydrodynamic damping matrix (NxN) [kg/s]
d	=	buoy draft [m]
D	=	buoy waterline diameter [m]
f	=	wave frequency [Hz]
F	=	force [N]
I	=	identity matrix (NxN) [-]
K	=	stiffness matrix (NxN) [kg/s^2]
H	=	wave height [m]
m	=	buoy mass [kg]
m_{sup}	=	supplementary mass [kg]
M	=	buoy mass matrix (NxN) [kg]
M_a	=	added mass matrix (NxN) [kg]
M_{sup}	=	supplementary mass matrix (NxN) [kg]
N	=	number of buoys [-]
n_f	=	number of frequencies [-]
q	=	ratio of maximum power absorption by N interacting bodies to N isolated bodies [-]
$\tilde{q}$	=	power absorption ratio of N interacting bodies and N isolated bodies in suboptimal conditions [-]
S	=	wave spectrum [m^{2}s]
t	=	time [s]
T	=	wave period [s]
z	=	buoy position [m]
Z	=	buoy position vector (Nx1)[m]
γ	=	peak enhancement factor [-]
ζ	=	wave elevation [m]
σ	=	spectral width parameter [-]
ω	=	angular frequency [rad^{-1}]

Subscripts

A	=	amplitude
abs	=	absorbed
ex	=	exciting
f	=	frequency
max	=	maximum value
p	=	peak value
s, $sign$	=	significant

1 Introduction

Point absorbers are oscillating wave energy converters with dimensions that are small compared to the incident wave lengths. In order to absorb a considerable amount of power, several point absorbers are grouped in one or more arrays. Some point absorber devices under development consist of a large structure containing multiple closely spaced oscillating bodies. Examples are Wave Star [1], Manchester Bobber [2] and FO^3 [3].

Several theoretical models dealing with interacting bodies have been developed. Budal [4], Evans [5] and Falnes [6] adopted the 'point absorber approximation' to derive expressions for the maximum power an array can absorb. The approximation relies on the assumption that the bodies are small compared to the incident wave lengths, so the wave scattering within the array can be neglected while calculating the interactions. A theory accounting more accurately for the body interactions is the 'plane-wave approximation' [7–9], which is based on the assumption that the bodies are widely spaced relative to the incident wavelengths, so the radiated and circular scattered waves can be locally approximated by plane waves. For closely spaced bodies, which is the focus of this paper, this theory is not suitable as the wide spacing requirement is not fulfilled, except for very short wave lengths. In the majority of studies, both theories have been applied to arrays for unconstrained conditions. Contrary to the point absorber approximation, the plane wave approximation is also suitable to study the power absorption of an array in suboptimal conditions, as scattering might be relatively important in that case [7, 10]. Heaving point absorbers with constraint displacements have been studied by McIver [10, 11] by means of the plane wave approximation and by Thomas and Evans [12] with the point absorber approximation, although less suitable. Motion restrictions appeared to significantly reduce the power absorption capability of the array for longer wave lengths [10]. Apart from regular waves, McIver et al. [11] also studied array interactions in irregular unidirectional and directionally spread seas for a varying number of oscillators between 5 and 20, arranged in one or two lines. For unconstrained motions constructive interactions between the point absorbers were observed for unidirectional irregular normal waves. When constraints were implemented this effect disappeared and in random seas it is almost non-existing in both unidirectional irregular waves and random seas.

More exact results on array hydrodynamics can be obtained by the 'multiple scattering' theory of Mavrakos [13]. This theory has been extensively compared with the above mentioned approximate theories (the point absorber approximation and plane wave approximation) [14, 15].

With current computer capacity, Boundary Element Methods (BEM) are becoming more and more important to investigate interacting point absorbers. Ricci et al. [16] compared results obtained with a BEM code to the point absorber approximation and optimized the point absorber geometry and interbody distance of two array configurations, each consisting of 5 floaters in irregular waves with and without directional spreading. Taghipour et al. [3] investigated the interaction of 21 heaving point absorbers in a floating platform, known as the FO^3 device, in unconstrained conditions. By means of a mode expansion method, he was able to reduce the computation time to calculate the body responses by a factor of 10 tot 15. Recently, numerical simulations predicting the response amplitude of the floater motions of interacting hemispherical floaters using the BEM package WAMIT [17] have been validated with experimental tests on line array configurations by Thomas et al. [12].

The impact of constraints on a single point absorber has been studied by De Backer et al. [18], showing that stroke and force restrictions might have a significant impact on the power absorption. In that paper the influence of slamming and stroke restrictions as well as limitations on the power take-off (PTO) forces are investigated for an array in a frequency domain model with WAMIT. The results are compared with the performance of an isolated buoy under the same restrictions. Apart from the total amount of power absorbed by multiple bodies, attention is paid to the individual power absorption and the difference in performance between the buoys within a certain configuration. The control parameters are optimized with different strategies, among them diagonal optimization and individual optimization.

2 Configuration

A configuration of 12 buoys in a staggered grid is considered, as shown in Fig. 1. The buoys are placed in a square, fixed structure with four supporting columns at the edges. However, the effects of diffraction and reflection of waves on the columns will be further neglected in this study. The interdistance between two successive rows is 6.5 m. The incoming waves propagate in the direction of the *x*-axis, as indicated in Fig. 1. The buoys are assumed to oscillate in heave mode only. In Fig. 2 the buoy geometry is presented. A buoy consists of a cone shape with apex angle 90° and a cylindrical upper part with a diameter of 5 m. The equilibrium draft of the buoy is 3 m.

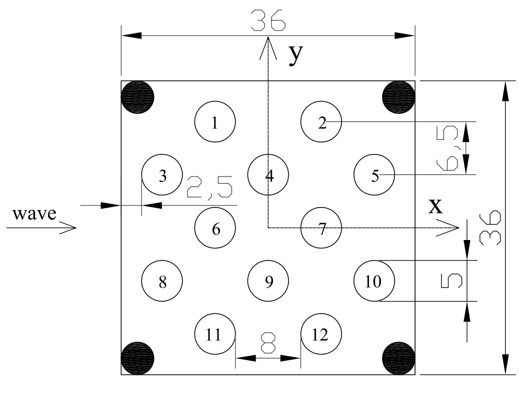

Figure 1: Multiple body configuration, dimensions in m.

3 Numerical modelling

3.1 Equation of motion

The equation of motion of an oscillating point absorber can be described by Newton's second law:

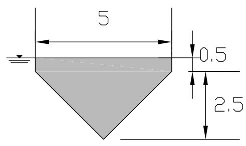

Figure 2: Point absorber layout, dimensions in m.

$$m\ddot{z} = F_{ex} + F_{rad} + F_{res} + F_{damp} + F_{tun} \quad (1)$$

where m is the mass of the buoy and $\ddot{z}$ its acceleration. F_{ex} is the exciting force, F_{rad} the radiation force, F_{res} the hydrostatic restoring force, F_{damp} the external damping force to extract power and F_{tun} the tuning force for phase-controlling the buoy. The latter two forces are to be delivered by the power take-off (PTO) system. For simplicity, the PTO is assumed linear.

The equation of motion of N multiple bodies, oscillating in heave in a regular wave with angular frequency ω, can be expressed as follows with linear theory in the frequency domain:

$$-\omega^2(\mathbf{M}+\mathbf{M_a}+\mathbf{M_{sup}})\hat{\mathbf{Z}}+j\omega(\mathbf{B_{ext}}+\mathbf{B_{hyd}})\hat{\mathbf{Z}}+\mathbf{K}\hat{\mathbf{Z}} = \hat{\mathbf{F}}_{\mathbf{ex}} \quad (2)$$

where $\hat{\mathbf{Z}}$ is the complex amplitude of the buoy positions, $\mathbf{M}$ the mass matrix of the buoys, and $\mathbf{K}$ the matrix with hydrostatic restoring coefficients or stiffness matrix. The added mass matrix and hydrodynamic damping matrix are denoted by $\mathbf{M_a}$ and $\mathbf{B_{hyd}}$, respectively. They are both symmetric N x N matrices with the hydrodynamic interaction coefficients on the non-diagonal positions. The vector $\hat{\mathbf{F}}_{\mathbf{ex}}$ contains the complex amplitudes of the heave exciting forces. The hydrodynamic parameters $\mathbf{M_a}$, $\mathbf{B_{hyd}}$ and $\hat{\mathbf{F}}_{\mathbf{ex}}$ are calculated with the Boundary Element Method (BEM) software WAMIT [17]. Since the natural frequency of the buoys is generally smaller than the incident wave frequencies, the buoys are often tuned towards the characteristics of the incident waves to augment power absorption. This can be effectuated by latching techniques [19], by introducing a supplementary spring term [16] or a supplementary mass term [20]. In this paper, a tuning force proportional to the acceleration has been implemented by means of a supplementary mass matrix, $\mathbf{M_{sup}} = m_{sup}^{(j)}\,\mathbf{I}$, with $m_{sup}^{(j)}$ the supplementary mass for buoy j and $\mathbf{I}$ the NxN identity matrix. In earlier experimental research the supplementary mass has been realized by adding masses on both sides of a rotating belt connected to the heaving point absorber [20, 21]. In that way the inertia of the system can be varied without changing the draft of the buoy. For practical applications, the tuning force, associated with the supplementary mass, is more likely to be realized by a control mechanism, e.g. by the PTO, rather than by adding real masses to the device. A linear external damping matrix, $\mathbf{B_{ext}} = b_{ext}^{(j)}\,\mathbf{I}$, has been applied, enabling power extraction.

The superposition principle is used to obtain the time-averaged power absorption in irregular waves [16]:

$$\mathbf{P_{abs}} = \sum_{i=1}^{n_f} \frac{1}{2}\omega_i^2 \mathbf{Z_i^*} \mathbf{B_{ext}} \mathbf{Z_i} \quad (3)$$

where n_f is the number of frequencies and $\mathbf{Z_i^*}$ the complex conjugate transpose of $\mathbf{Z_i}$. The calculations are performed for 40 frequencies, ranging between 0.035 and 0.300 Hz. All buoys are assumed to be equipped with their own power take-off system.

3.2 Constraints

Slamming constraint

Slamming is a phenomenon that occurs when the buoy re-enters the water, after having lost contact with the water surface. The buoy experiences a slam, which may result in very high hydrodynamic pressures and loads. These impacts have a very short duration, with a typical order of magnitude of milliseconds. However, they may cause local plastic deformation of the material [22]. Fatigue by repetitive slamming pressures can be responsible for structural damage of the material. For this reason, a restriction has been implemented, requiring that the significant amplitude of each buoy position relative to the free water surface elevation should be smaller than a fraction α of the draft d of the buoy:

$$(z^{(j)} - \zeta^{(j)})_{A,sign} \leq \alpha \cdot d \quad (4)$$

where $z^{(j)}$ is the position of buoy j, $\zeta^{(j)}$ the water elevation at the center of buoy j and α a parameter that is arbitrarily chosen equal to one. The water elevation has been determined with the incident wave only, thereby neglecting the radiated and diffracted waves from the buoys.

This slamming restriction might require a decrease of the tuning parameter m_{sup} and/or an increase of the external damping coefficient b_{ext}. Not only the occurrence probability of slamming will be reduced by this measure, but also the magnitude of the associated impact pressures and loads will drop, since they are dependent on the impact velocity of the body relative to the water particle velocity and this impact velocity will decrease when the control parameters of the buoy are adapted according to the restriction imposed.

Stroke constraint

In practice, many point absorber devices are very likely to have restrictions on the buoy motion, e.g. imposed by the limited height of the rams in case of a hydraulic conversion system or by the limited height of a platform structure enclosing the oscillating point absorbers. Therefore a stroke constraint is implemented, imposing a maximum value on the significant amplitude of the body motion:

$$z_{A,sign}^{(j)} \leq z_{A,sign,max}^{(j)} \quad (5)$$

With the position spectrum defined as: $S_{z_i}^{(j)} = z_{A,i}^{(j)2}/2\Delta f$, the significant amplitude of the buoy motion can be obtained from $z_{A,sign} = 2\sqrt{\int_{i=1}^{n_f} S_{z,i}^{(j)} \cdot \mathrm{d}f}$. Hence, the constraint on the significant amplitude of the buoy motion is not an absolute constraint, but a restriction associated with a statistical exceedance probability. In the examples that will be presented in this paper, a maximum value of the significant amplitude of 2.00 m is chosen. Assuming Rayleigh distribution of the buoy motions, this restriction means that a stroke of 4.90 m is exceeded for 5.0 % of the waves. The implementation of constraints on the body motion increases the reliability of the linear model, which is based on the assumption of small body motions.

Force constraint

In some cases, the optimal control parameters for maximum power absorption, result in very large control forces. The tuning force, in particular, might become very high and can even be a multiple of the damping force. If this tuning force is to be delivered by the PTO, it might result in a very uneconomic design of the PTO system. For this reason it is interesting to study the response of the floaters in case the total control force is restricted. If the force spectrum is expressed as: $S_{F,i}^{(j)} = F_{A,i}^{(j)2}/2\Delta f$ and the significant amplitude of the force is defined as $F_{A,sign}^{(j)} = 2\sqrt{\int_{i=1}^{n_f} S_{F,i}^{(j)} \cdot \mathrm{d}f}$, then the significant amplitude of the damping and tuning force, respectively, for buoy j are given by:

$$F_{bext,A,sign}^{(j)} = 2\sqrt{\int_0^\infty S_{F_{bext,A}}^{(j)}(f)\mathrm{d}f} \tag{6}$$

$$F_{msup,A,sign}^{(j)} = 2\sqrt{\int_0^\infty S_{F_{msup,A}}^{(j)}(f)\mathrm{d}f} \tag{7}$$

A restriction will be imposed on the significant amplitude of the total force, expressed as:

$$F_{tot,A,sign}^{(j)} = 2\sqrt{\int_0^\infty \left(S_{F_{bext,A}}^{(j)}(f) + S_{F_{msup,A}}^{(j)}(f)\right)\mathrm{d}f} \tag{8}$$

Simulation results will be presented where $F_{tot,A,sign}^{(j)}$ is limited to 100 kN and 200 kN.

3.3 Wave climate

Scatter diagrams based on buoy measurements at Westhinder, on the Belgian Continental Shelf, have been used to define nine sea states with their corresponding occurrence probabilities (OP), see Table 1. Westhinder is located 32 km from shore and has a mean water depth of 28.8 m. The majority of calculations will be carried out for the fifth sea state, characterized by a significant wave height, H_s = 2.25 m and peak period, T_p = 7.22 s. The generated spectrum is based on a parameterized JONSWAP spectrum [23].

Table 1: Sea states and occurrence probabilities at Westhinder based on measurements from 1-7-1990 until 30-6-2004 (Source of original scatter diagram: Flemish Ministry of Transport and Public Works (Agency for Maritime and Coastal Services Coastal Division))

Sea state	H_s [m]	T_p [s]	OP [%]
1	0.25	5.24	21.58
2	0.75	5.45	37.25
3	1.25	5.98	22.02
4	1.75	6.59	10.65
5	**2.25**	**7.22**	**5.14**
6	2.75	7.78	2.27
7	3.25	8.29	0.79
8	3.75	8.85	0.21
9	4.25	9.10	0.07

4 Optimization strategies

The relative performance of an array is often expressed by means of the 'q-factor', defined as the maximum possible time-averaged total power absorbed by the N bodies in the array devided by N times the maximum time-averaged power absorption by a single point absorber.

$$q = \frac{P_{\text{abs, max by array of } N \text{ floaters}}}{N \cdot P_{\text{abs, max by an isolated floater}}} \tag{9}$$

Since the control matrices are diagonal matrices and the control parameters are optimized for a certain sea state, rather than for a particular frequency, the power absorption will be suboptimal, even in unconstrained conditions. Hence, for the current purpose, a measure is needed to express and compare the efficiency of different optimization strategies applied to a given array in suboptimal conditions. Therefore a gain factor $\tilde{q}$ is defined as the ratio of the total power absorbed by the array to the power absorbed by the point absorbers in isolation, subjected to the same constraints.

Three strategies to determine the control parameters for multiple bodies will be compared: optimal control parameters from a single body, diagonal optimization and individual optimization.

Optimal control parameters from a single body

In the first strategy, the optimal control parameters from a single body (OPSB) are applied to all the bodies in the array. It should be kept in mind that optimal parameters in this case means that these parameters lead to the maximum possible power absorption within the imposed constraints and with the described linear PTO and hence they do not necessarily give the absolute maximum power absorption of the array. With this method all bodies have the same control coefficients. However, the control forces, $M_{sup}\ddot{Z}$ and $B_{ext}\dot{Z}$, are not similar for the different buoys, since the buoy velocities and accelerations differ in amplitude and phase. If m_{sup} and b_{ext} are the single body optimal parameters for a specific sea state and a certain combination of restrictions, then the absorbed power for the array is obtained with the following power take-off matrices:

$$\mathbf{M_{sup}} = m_{sup}\,\mathbf{I} \; and \; \mathbf{B_{ext}} = b_{ext}\,\mathbf{I} \tag{10}$$

Diagonal optimization

With the second technique all the buoys still get the same parameters, but they are optimized with a simplex search (SS) method for unconstrained conditions and a sequential quadratic programming (SQP) method for constrained conditions. The methods are validated with an exhaustive searching (ES) method. The latter method gives the same results as SS and SQP, however, SS and SQP are much faster if very accurate results need to be obtained. The supplementary mass matrix and external damping matrix are similar as those in Eq. 10, but m_{sup} and b_{ext} are determined so that the total absorbed power is maximal for the specific array. This technique is called diagonal optimization (DO) [16].

Individual optimization

With the last technique the floaters are individually optimized (IO), i.e. for every floater seperate values of $m_{sup}^{(j)}$ and $b_{ext}^{(j)}$ are determined. IO has only been successfully applied in constrained conditions. The optimization is carried out with a SQP method only, since a simple exhaustive searching method would require too much CPU-time. If $n_{m_{sup}}$ and $n_{b_{ext}}$ values of $m_{sup}^{(j)}$ and $b_{ext}^{(j)}$, respectively, are to be evaluated, the total power absorption need to be calculated $(n_{m_{sup}} \cdot n_{b_{ext}})^{12}$ times. If e.g. 40 values for each control parameter are to be assessed, $2.8 \cdot 10^{38}$ power absorption calculations would be required, which is not feasible. A drawback of the SQP algorithm for individual tuning is that it might converge to a local maximum, depending on the initial conditions. Hence, the choice of the initial conditions is very important. Here, the control parameters from diagonal optimization have been used as initial values from which individual tuning parameters are obtained. If the number of buoys were smaller (preferably smaller than 6), the SQP algorithm could be executed with a set of initial conditions for $m_{sup}^{(j)}$ and $b_{ext}^{(j)}$ (multistart algorithm) to increase the chance of reaching the absolute maximum value. Unfortunately, a multistart application is much too time-consuming for twelve buoys, even if only two initial values per parameter are selected.

5 Results

5.1 Unconstrained

In this section, simulations are presented for unconstrained point absorber motions and control forces. Fig. 3(a) shows the time-averaged power absorption for each floater. As expected, the diagonal optimization (DO) method is more efficient than applying the optimal parameters of a single buoy to the array (OPSB). The power absorption is distributed very unequally between the buoys: the front buoys (in particular Nos 3 and 8) absorb about 2.7 times more energy than the buoy No 7 in the back. Rather large buoy motions are observed in Fig. 3(b), showing the significant amplitudes of the position of the buoys. Figs. 4(c) and 4(d) present the external damping coefficients and supplementary mass coefficients, respectively.

If diagonal optimization is applied, the total power absorption is ca 400 kW. This corresponds to an increase with almost 50 kW compared to OPSB, as can be observed in Table 2. Although the power absorption of the array is large, the gain factor $\tilde{q}$ is rather small (46%), since the absorbed power of an isolated buoy is quite high. It must be stressed, however, that this unconstrained case leads to unpractically large control forces (up to a value of $F_{tot,A,sign}$ of 400 kN) and floater motions, violating the assumptions behind linear theory. Consequently, these power absorption figures will most likely not be achieved in practical cases. Furthermore the power absorption figures do not take into account losses due to mechanical friction, turbulence losses, turbine and generator losses or any other losses in the conversion system and are for that reason not equal to the produced electrical power.

In unconstrained conditions, an individual tuning (IO) did not lead to any realistic solutions. Some buoys may be totally tuned towards resonance, oscillating with extremely large amplitudes, while other buoys are kept still. This is of course not a desired situation at all. Moreover, in unconstrained conditions the optimization algorithm has a large chance to find a local maximum instead of the absolute maximum, sometimes even without finding a solution which is symmetric with respect to the x-axis. More realistic, constrained cases will be addressed in the next section.

5.2 Constrained

5.2.1 Slamming and Stroke constraint

The power absorption and gain factor are determined for the three optimization strategies, taking into account the slamming and stroke restrictions, as explained in section 3.2. Table 2 shows that diagonal optimization performs slightly better than the optimal parameters of a single body: the total power absorption is 381 kW with OPBS and 389 kW with DO. A significant benefit can be made by individually optimizing the control parameters of the floaters. The power absorption becomes 443 kW with IO, which is an increase of about 14 % compared to DO or an increase of 54 kW. This figure corresponds with the amount of power produced by an isolated buoy, and illustrates the large profit than can be made by individually tuning the buoys in case they are closely spaced. For the configurations evaluated in [16], the benefit of IO compared to DO was found to be less than one percent. This is most probably due to the fact that the floaters are wider spread from each other in

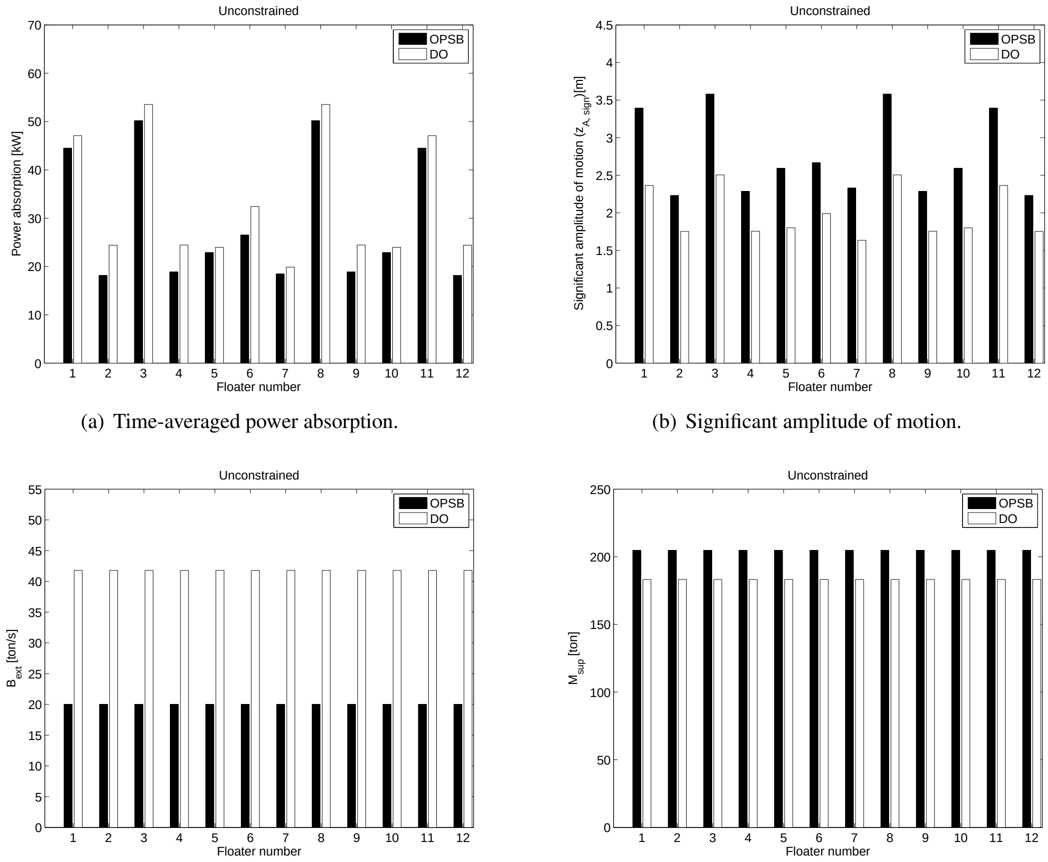

(a) Time-averaged power absorption.

(b) Significant amplitude of motion.

(c) External damping coefficients.

(d) Supplementary mass coefficients.

Figure 3: Simulation results in unconstrained conditions, with optimal control parameters for a single body and diagonal optimization.

[16]. The interdistance (center-center spacing) between two successive rows, for which the two methods were evaluated, varied between 3 and 4 times the diameter *D*, whereas in the present configuration the interdistance is about 1.3 *D*. The larger the interdistance, the more the buoy behaviour resembles that of an isolated buoy and the less difference will be found between the different techniques. Also the number of floaters is much smaller in [16]: five floaters are considered compared to twelve floaters in the present configuration. Particularly, the buoys in the back benefit considerably from an individual tuning, as is shown in Fig. 4(a), presenting the power absorption for each buoy. With IO, the power absorption is much better distributed among the floaters. A maximum factor of 2.6 is found between the individual power absorption of the front buoys and the rear buoys if DO is used, whereas only a factor of 1.9 is observed when IO is utilized. With individual optimisation the buoys in the front absorb less power than with OPSB or DO, however, the buoys in the back become more efficient. This is realized by detuning the front buoys (small value of m_{sup}) and increasing their damping (larger value of b_{ext}) (Figs. 4(c)-4(d)). The rear buoys, on the other hand, are tuned very well to increase their velocity amplitude and power absorption. Consequently, the power that is not absorbed anymore by the front buoys can be absorbed by the buoys in the rows behind them. This makes the influence of restrictions less drastic for an array than for a single buoy. These conclusions will be even more pronounced when the constraints are stricter, as they will be in the next sections.

All the buoys reach the maximum stroke value, so the stroke restriction is dominant (Fig. 4(b)). The slamming constraint will generally not be critical in the presented examples for the given buoy dimensions and sea state.

5.2.2 Slamming, stroke and mild force constraint

In this section the slamming and stroke restrictions are included together with a force constraint of 200 kN on the significant amplitude of the total control force. Figs. 5(a)-5(d) give the power absorption, significant amplitude of the motion and the control parameters of each buoy. The significant amplitude of the damping force, tuning force and total force are presented in Figs. 5(e)-5(g) for the three optimization methods. The force constraint is clearly the most critical constraint. The buoy motions are considerably smaller than the stroke limit. The force limit on the other hand, is reached by the front buoys with the OPSB and DO methods and by all the buoys with IO. The front buoys even exceed the limit of 200 kN in case of OPSB. If certain

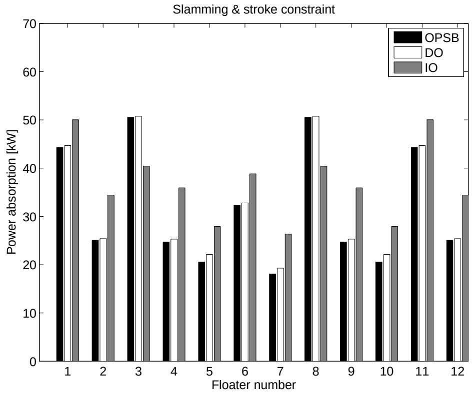

(a) Time-averaged power absorption.

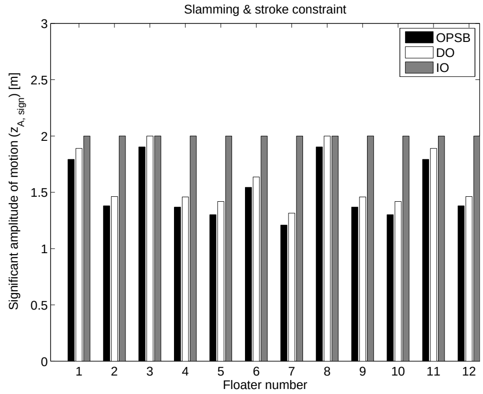

(b) Significant amplitude of motion.

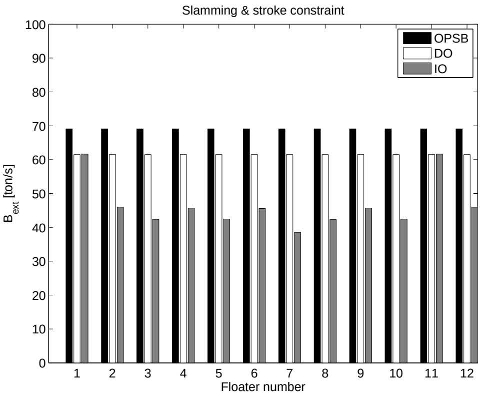

(c) External damping coefficients.

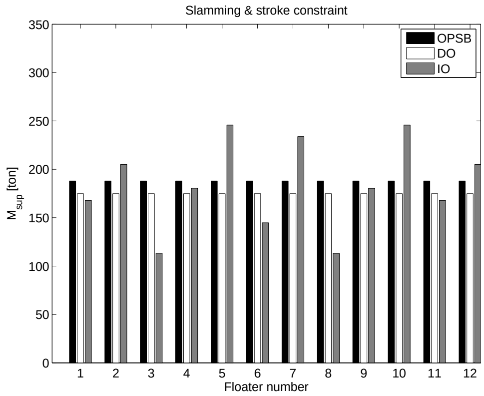

(d) Supplementary mass coefficients.

Figure 4: Simulation results in constrained conditions (slamming and stroke restriction), with optimal control parameters for a single body, diagonal and individual optimization.

control parameters meet the constraints for an isolated buoy, they do not necessarily satisfy the same restrictions applied to an array. This explains why more power is absorbed with OPSB (336 kW) than with the DO method (332 kW) in this case (see Table 2), although the DO method was found to be more efficient. Again, a large benefit can be made with the IO technique: the power absorption becomes 379 kW, corresponding with an increase of 46 kW compared to DO, which is even more than the power absorbed by an isolated buoy under the same constraints. Due to the extra force constraint, the power distribution among the floaters has again been improved compared to the previous case; the buoys in the front absorb about 50% more than those in the back with IO and about double as much than the rear buoys if DO is employed. The gain factors $\tilde{q}$ have risen to 0.69 and 0.79 for this restriction case, although the total power absorption of the array has decreased due to the extra force constraint. This rise of $\tilde{q}$ can be attributed to the considerable power drop by an isolated buoy under these restrictions. An isolated buoy loses about 25 % of the power absorption, whereas the array loses only 12 to 14 % compared to the slamming and stroke restriction case. Since the array suffers a bit less from the constraints than the isolated buoy, it has an increased relative performance, although the absolute performance is decreased.

5.2.3 Slamming, stroke and strong force constraint

In this case, the same slamming and stroke constraints are applied, but the force constraint has been increased till a maximum value of 100 kN. Figs. 6(a)-6(g) show the simulation results of this test case. The power absorption seems to be considerably decreased with this restriction, but it is more equally distributed among the floaters. The largest difference between the power absorption of the front and rear buoys is a only factor of 1.7 and 1.4 with DO and IO, respectively. In order to satisfy this strong force restriction, phase control of the buoys is very limited. The tuning forces are considerably small in this case, even smaller than the damping forces.

Again, the restriction is not perfectly fulfilled with the OPSB method. With IO, all floaters have reached the maximum value of the total force, so it is very likely that the IO method has given the correct, most optimal solution. This strong force restriction has a harmful influence on the total power absorption, as displayed in Table 2. Compared to the previous case with the mild force constraint, the absorbed power drops with more than 40% for the single buoy and with 31% to 33% for the array.

The results in Table 2 for the different restriction combinations illustrate the benefits of phase control on power absorption. However, an economic optimum needs to be found between the power absorption profit of phase control and the costs to realise this tuning and to allow e.g. a larger stroke. Since the power absorption for an isolated buoy is very small, the gain factor reaches quite large values, up to 0.88. In other words the array has a good relative performance, since the rear buoys are still able to absorb an important share in the power, compared to an isolated buoy.

5.2.4 Angle of wave incidence and effects of mistuning

So far, irregular waves propagating along the x-axis have been considered. It might be of interest to investigate the array behaviour for a different angle of wave incidence β_i, e.g. $\beta_i = 45°$. In that case, the configuration in Fig. 1 can be considered as an aligned grid. The power absorption values and gain factors are presented in Table 2 for unconstrained motion as well as for the combination of slamming, stroke and mild force restrictions. It appears that the array performs slightly better when the incident waves propagate in the direction of the diagonal of the array (aligned grid), compared to normal incidence (staggered grid), however, the difference is not significant. The performance of an array is strongly dependent on the wave frequency and therefore the power absorption is calculated for the other sea states at Westhinder (as defined in Table 1). In Fig. 7 the gain factor $\tilde{q}$ for DO and IO is shown versus the sea state. A steep rise in $\tilde{q}$-factor can be noticed from sea state 4 onwards. This might give the impression that the gain factor rises for longer waves. However, the increase is most probably caused by the constraints, which become important for the more energetic wave classes. Since a single body is relatively more affected by the constraints, the gain factor rises in larger waves.

In Fig. 7 the difference between an angle of incidence of 0° and 45° is very minor for all sea states and no final conclusion can be made about the best angle of incidence. The difference in optimization strategy, on the other hand is very clear: for all sea states and both angles of incidence, individual optimization outperforms diagonal optimization.

In practise, there will be uncertainties on the characteristics of the sea state and the real sea state might not perfectly correspond to the values used in the numerical calculations. E.g. the real spectrum might differ from the JONSWAP spectrum that has been employed, the current angle of wave incidence might not be known exactly, etc. Hence, it is important to know the sensibility of the optimization techniques to mistuning effects. An example is given in Table 3 for unconstrained motion and one case of constrained conditions. Simulation results are presented for an angle of incidence of 45°, but the optimal control parameters are taken from the simulations with normal wave incidence. It is expected that for the individually optimized parameters the effect of mistuning will be

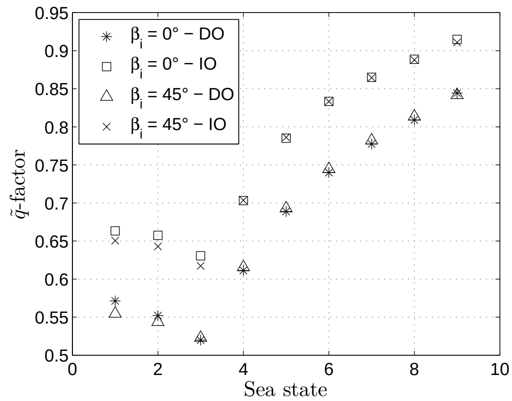

Figure 7: $\tilde{q}$-factors for diagonal and individual optimization as a function of the nine sea states on the Belgian Continental Shelf.

more pronounced than for the diagonally optimized parameters. This appears to be correct, however, the effect of mistuning is extremely small. For DO the difference in power absorption is less than 0.50% compared to the results with the correct control parameters for $\beta_i = 45°$. For IO this difference is 1.76% for the studied case. Obviously, the larger the mistuning, the larger will be the impact on the power absorption, in particular for IO. It needs to be mentioned that with the mistuned parameters, the force constraint is still fulfilled for DO, but not anymore for IO. The problem is caused by buoy No 12, exceeding the force limit by 20%. The buoy is tuned as a rear buoy ($\beta_i = 0°$), getting a high value of the supplementary mass, and becomes rather a front buoy when $\beta_i = 45°$, where it is subjected to higher incident waves. The combination of an increased supplementary mass and large buoy motion parameters leads to larger control forces.

6 Conclusion

The behaviour of twelve closely spaced point absorbers in unconstrained and constrained conditions has been analysed in irregular unidirectional waves. The buoys are assumed to be equipped with a linear power take-off, consisting of a linear damping and a linear tuning force. In unconstrained conditions the absorbed power is found to be very unequally distributed among the floaters. For the considered sea state, the front buoys absorbed 2.7 times more power than the rear buoys in unconstrained conditions. For the strongest constraints the difference was reduced to a factor of 1.4 to 1.7. The total power absorption of the array is negatively affected by the implementation of constraints. However, it is observed that the relative power loss of the array is less than for a single body, since mainly the front buoys are affected by the constraints and to a lesser extent the rear buoys. The power absorption of the array has been determined in three different ways. Firstly, the optimal parameters of a single body are applied to the array. This turns out not to be an efficient way. Moreover, the constraints were not always fulfilled for all the bodies

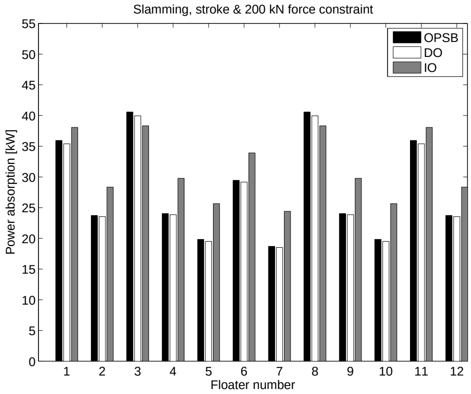

(a) Time-averaged power absorption.

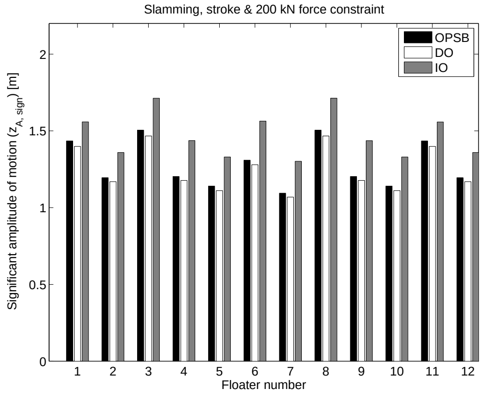

(b) Significant amplitude of motion.

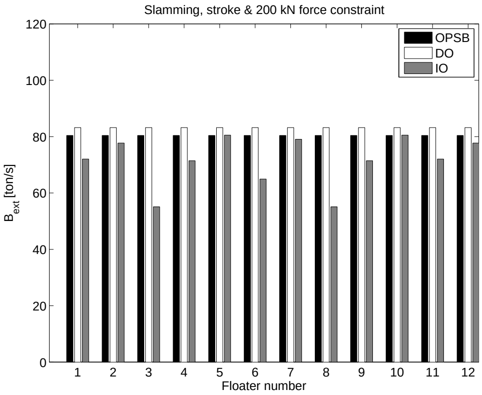

(c) External damping coefficients.

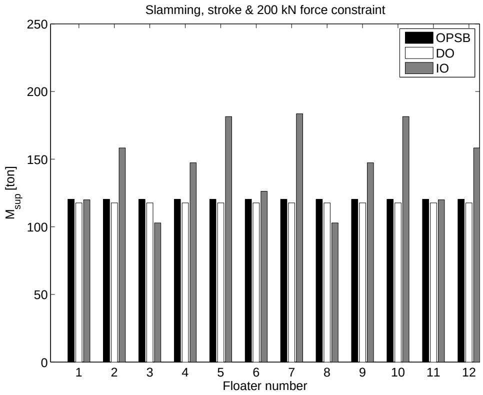

(d) Supplementary mass coefficients.

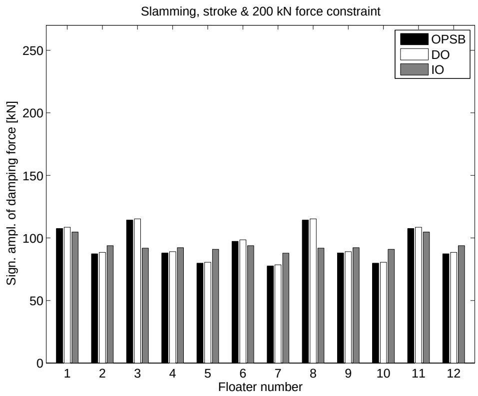

(e) Significant amplitude of damping force.

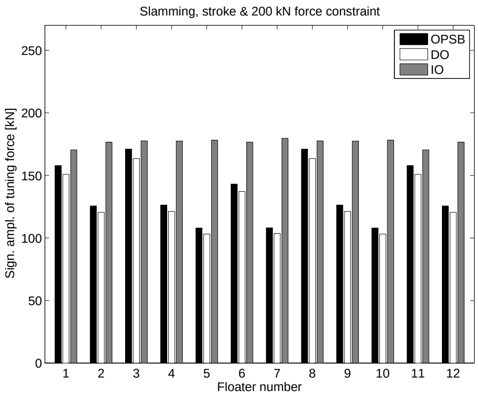

(f) Significant amplitude of tuning force.

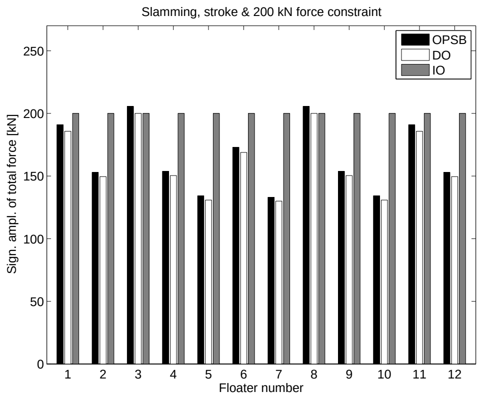

(g) Significant amplitude of total control force.

Figure 5: Simulation results in constrained conditions (slamming and stroke restriction, and mild force restriction: $F^{(j)}_{tot,A,sign} \leq$ 200 kN), with optimal control parameters for a single body, diagonal and individual optimization.

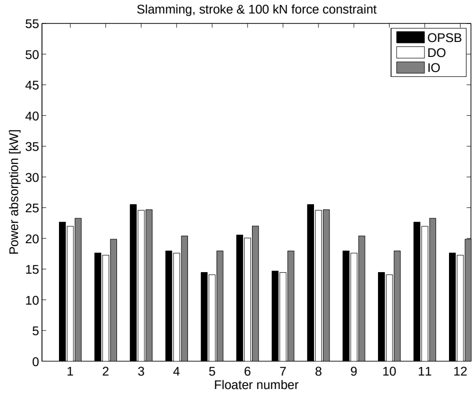

(a) Time-averaged power absorption.

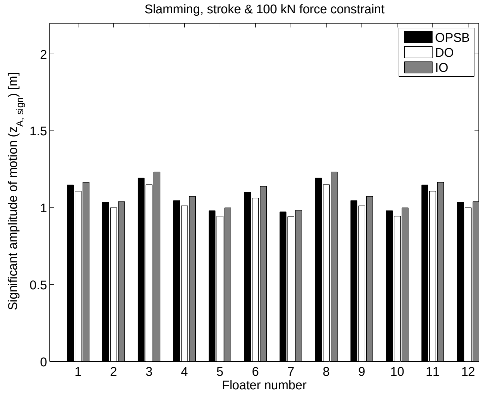

(b) Significant amplitude of motion.

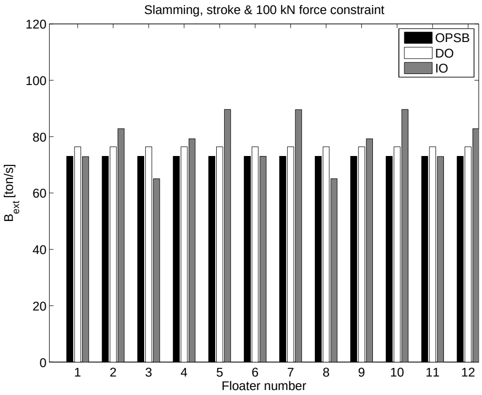

(c) External damping coefficients.

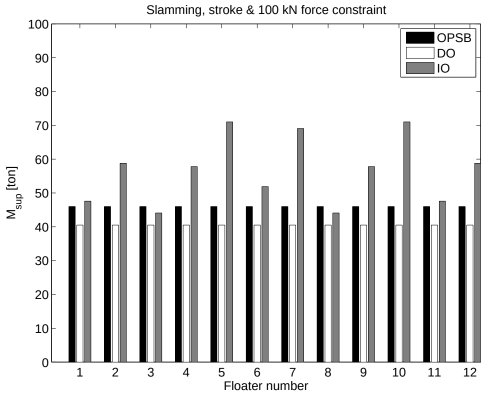

(d) Supplementary mass coefficients.

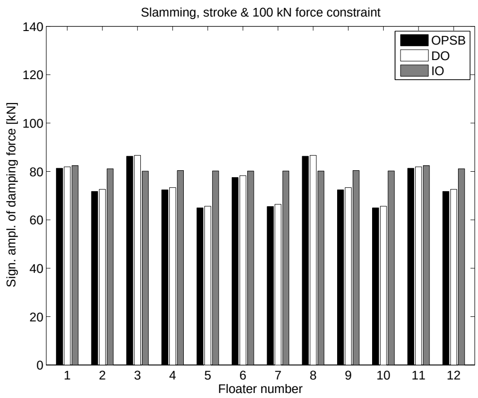

(e) Significant amplitude of damping force.

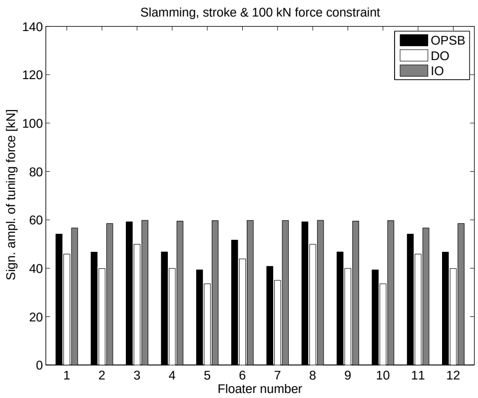

(f) Significant amplitude of tuning force.

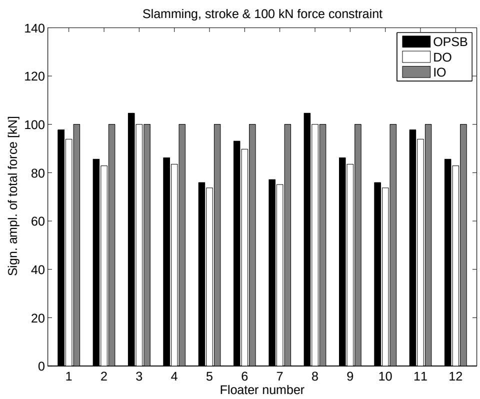

(g) Significant amplitude of total control force.

Figure 6: Simulation results in constrained conditions (slamming and stroke restriction, and strong force restriction: $F^{(j)}_{tot,A,sign} \leq$ 100 kN), with optimal control parameters for a single body, diagonal and individual optimization.

Table 2: Absorbed power and gain factor $\tilde{q}$ for unconstrained and constrained cases.

Sea state:	Single body (SB)	Multiple bodies (MB)					
H_s = 2.25 m, T_p = 7.22 s		OPSB		DO		IO	
Constraints	NP_{abs} [kW]	P_{abs} [kW]	$\tilde{q}$ [-]	P_{abs} [kW]	$\tilde{q}$ [-]	P_{abs} [kW]	$\tilde{q}$ [-]
$\beta_i = 0°$							
Unconstrained	872	354	0.41	399	0.46	-	-
Slam, stroke 2.00 m	645	381	0.59	389	0.60	443	0.69
Slam, stroke 2.00 m, force 200 kN	482	336	0.70	332	0.69	379	0.79
Slam, stroke 2.00 m, force 100 kN	286	232	0.81	225	0.79	252	0.88
$\beta_i = 45°$							
Unconstrained	872	360	0.41	403	0.46	-	-
Slam, stroke 2.00 m, force 200 kN	482	337	0.70	334	0.69	379	0.79

Table 3: Effects of mistuning - power absorption for $\beta_i = 45°$, while the control parameters (CP) are those obtained for $\beta_i = 0°$.

Sea state:						
H_s = 2.25 m, T_p = 7.22 s	DO			IO		
Constraints	P_{abs} [kW]	$\tilde{q}$ [-]	Power loss [%]	P_{abs} [kW]	$\tilde{q}$ [-]	Power loss [%]
$\beta_i = 45°$, CP from $\beta_i = 0°$						
Unconstrained	403	0.46	0.01	-	-	
Slam, stroke 2.00 m, force 200 kN	333	0.69	0.45	372	0.77	1.76

in the array, although they were satisfied for the single body case. Secondly, diagonal optimization has been applied. With this method all buoys have the same control parameters, but they are optimized for the array. In the third method, the buoys get individually optimized control parameters. This strategy clearly outperforms the two other methods. By individually optimizing the control parameters, the power absorption was on average increased by 14 %, compared to diagonally optimizing them.

Acknowledgements

Research funded by Ph.D. grant of the Institute of Promotion of Innovation through Science and Technology in Flanders (IWT-Vlaanderen), Belgium.

References

[1] A. Bjerrum. The wave star energy concept. In *2nd International Conference on Ocean Energy*, 2008.

[2] http://www.manchesterbobber.com/.

[3] R. Taghipour, A. Arswendy, M. Devergez, and T. Moan. Efficient frequency-domain analysis of dynamic response for the multi-body wave energy converter in multi-directional waves. In *The 18th International Offshore and Polar Engineering Conference*, 2008.

[4] K. Budal. Theory for absorption of wave power by a system of interacting bodies. *Journal of Ship Research*, 21:248–253, 1977.

[5] D.V. Evans. *Some analytic results for two- and three-dimensional wave-energy absorbers*. B. Count: Academic Press, 1980.

[6] J. Falnes. Radiation impedance matrix and optimum power absorption for interacting oscillators in surface waves. *Applied Ocean Research*, 2:75–80, 1980.

[7] J. Simon. Multiple scattering in arrays of axisymmetric wave-energy devices. part 1. a matrix method using a plane-wave approximation. *Journal of Fluid Mechanics*, 120:1–25, 1982.

[8] P. McIver and D. Evans. Approximation of wave forces on cylinder arrays. *Applied Ocean Research*, 6:101–107, 1984.

[9] P. McIver. Wave forces on arrays of bodies. *Journal of Engineering and Mathematics*, 18:273–285, 1984.

[10] P. McIver. Some hydrodynamic aspects of arrays of wave-energy devices. *Applied Ocean Research*, 16:61–69, 1994.

[11] P. McIver, S. A. Mavrakos, and G. Singh. Wave-power absorption by arrays of devices. In *2nd European Wave Power Conference*, pages 126–133, Portugal, 1995.

[12] S. Thomas, S. Weller, and T. Stallard. Comparison of numerical and experimental results for the response of heaving floats within an array. In *2nd International Conference on Ocean Energy*, France, 2008.

[13] S. A. Mavrakos. Hydrodynamic coefficients for groups of interacting vertical axisymmetric bodies. *Ocean Engineering*, 18:485–515, 1991.

[14] S.A. Mavrakos and A. Kalofonos. Power absorption by arrays of interacting vertical axisymmetric wave-energy devices. *Journal of Offshore Mechanics and Artic Engineering - Transactions of the ASME*, 119:244–251, 1997.

[15] S. A. Mavrakos and P. McIver. Comparison of methods for computing hydrodynamic characteristics of arrays of

wave power devices. *Applied Ocean Research*, 19:283–291, 1997.

[16] P. Ricci, J.-B. Saulnier, and A.F. Falc ao. Point-absorber arrays: a configuration study off the Portuguese west-coast. In *7th European Wave and Tidal Energy Conference*, Portugal, 2007.

[17] Wamit user manual: http://www.wamit.com/manual.htm.

[18] G. De Backer, M. Vantorre, R. Banasiak, J. De Rouck, C. Beels, and H. Verhaeghe. Performance of a point absorber heaving with respect to a floating platform. In *7th European Wave and Tidal Energy Conference*, Portugal, 2007.

[19] K. Budal and J. Falnes. *Interacting point absorbers with controlled motion, in Power from Sea Waves*. B. Count: Academic Press, 1980.

[20] M. Vantorre, R. Banasiak, and R. Verhoeven. Modelling of hydraulic performance and wave energy extraction by a point absorber in heave. *Applied Ocean Research*, 26:61–72, 2004.

[21] G. De Backer, M. Vantorre, K. De Beule, C. Beels, and J. De Rouck. Experimental investigation of the validity of linear theory to assess the behaviour of a heaving point absorber at the belgian continental shelf. In *submitted to the 28th International Conference on Ocean, Offshore and Arctic Engineering*, Hawaii, 2009.

[22] B. Peseux, L. Gornet, and B. Donguy. Hydrodynamic impact : Numerical and experimental investigations. *Journal of Fluids and Structures*, 21(3):277–303, 2005.

[23] Z. Liu and P. Frigaard. Random seas. Aalborg University, 1997.